# Sirt1 Is a Regulator of Bone Mass and a Repressor of *Sost* Encoding for Sclerostin, a Bone Formation Inhibitor

Einav Cohen-Kfir, Hanna Artsi, Avi Levin, Eva Abramowitz, Alon Bajayo, Irina Gurt, Lei Zhong, Agustina D'Urso, Debra Toiber, Raul Mostoslavsky, and Rivka Dresner-Pollak

Department of Medicine, Endocrinology and Metabolism Service (E.C.-K., H.A., A.L., E.A., I.G., R.D.-P.), Hadassah-Hebrew University Medical Center, Jerusalem 91120, Israel; Bone Laboratory (A.B.), Hebrew University of Jerusalem, Jerusalem 91120, Israel; and the Massachusetts General Hospital Cancer Center (L.Z., A.D., D.T., R.M.), Harvard Medical School, Boston, Massachusetts 02114

Sirt1, the mammalian ortholog of the yeast Sir2 (silent information regulator 2), was shown to play an important role in metabolism and in age-associated diseases, but its role in skeletal homeostasis and osteoporosis has yet not been studied. Using 129/Sv mice with a germline mutation in the *Sirt1* gene, we demonstrate that *Sirt1* haplo-insufficient (*Sirt1*$^{+/-}$) female mice exhibit a significant reduction in bone mass characterized by decreased bone formation and increased marrow adipogenesis. Importantly, we identify *Sost*, encoding for sclerostin, a critical inhibitor of bone formation, as a novel target of Sirt1. Using chromatin immunoprecipitation analysis, we reveal that Sirt1 directly and negatively regulates *Sost* gene expression by deacetylating histone 3 at lysine 9 at the *Sost* promoter. *Sost* down-regulation by small interfering RNA and the administration of a sclerostin-neutralizing antibody restore gene expression of osteocalcin and bone sialoprotein as well as mineralized nodule formation in *Sirt1*$^{+/-}$ marrow-derived mesenchymal stem cells induced to osteogenesis. These findings reveal a novel role for Sirt1 in bone as a regulator of bone mass and a repressor of sclerostin, and have potential implications suggesting that Sirt1 is a target for promoting bone formation as an anabolic approach for treatment of osteoporosis. (*Endocrinology* **152: 4514–4524, 2011**)

The sirtuins are a family of evolutionarily highly conserved protein deacetylases that were found to regulate the life span in lower species and key cellular and metabolic functions in mammals (1). Sirtuin 1 (Sirt1), a nicotinamide adenine dinucleotide-dependent deacetylase and the mammalian homolog of yeast silent information regulator 2 (Sir2), was first identified based on its role in chromatin remodeling associated with gene silencing and prolonged life span (2). It was then shown to mediate the life-extending effect of calorie restriction, the regimen most consistently demonstrated to retard aging and extend longevity (3). Initially thought to be a histone

deacetylase only, Sirt1 is now known to be present in both the cytosol and the nucleus in which it deacetylates a host of nonhistone-regulatory proteins and transcription factors, such as p53, peroxisomal proliferator-activated receptor-γ coactivator-1α, p300, Forkhead box protein O1, nuclear factor-κB, and others (1). Although it is still unclear whether Sirt1 regulates the life span in mammals, overexpression of Sirt1 in mice confers protection against age-associated diseases such as obesity, diabetes (4), and Alzheimer's disease (5).

The role of Sirt1 in bone biology and osteoporosis has yet not been fully studied. Reduced Sirt1 protein level ac-

Abbreviations: BM-MSC, Bone marrow stromal mesenchymal stem cell; BV/TV, bone volume fraction; ChIP, chromatin immunoprecipitation; CrossLaps, C terminal telopeptides; μCT, microcomputed tomography; ES, embryonic stem; H3K9, histone 3 at lysine 9; LRP5, low-density lipoprotein receptor-related protein 5; PPAR, peroxisome proliferative-activated receptor; Sir2, silent information regulator 2; siRNA, small interfering RNA; Sirt1, sirtuin 1; WT, wild type.

companied by increased marrow adipogenesis was found in the bone marrow of ovariectomized mice and could be reversed upon estradiol administration (6). Resveratrol, a Sirt1 activator, was shown to increase osteoblastogenesis, reduce marrow adipogenesis, and decrease osteoclastogenesis *in vitro* (7–10). In addition, resveratrol was shown to preserve bone mineral density in elderly mice *in vivo* (11). However, resveratrol was also found to activate estrogen receptor-$\alpha$ and -$\beta$ as well as MAPK (12, 13). Thus, the reported effects may not reflect Sirt1 activity exclusively.

To investigate the role of Sirt1 in bone, we sought to characterize the skeletal phenotype in *Sirt1*-deficient mice. These mice bare a deletion of *Sirt1* exon 4, which encodes for the Sirt1 catalytic domain, *Sirt1*$^{\Delta ex4/\Delta ex4}$ (14). General *Sirt1* ablation in mice results in a high degree of postnatal lethality and severe malformations (14, 15). *Sirt1* haplo-insufficient *Sirt1*$^{+/\Delta ex4}$ (*Sirt1*$^{+/-}$) inbred 129/Sv mice are reported to be phenotypically normal but have an abnormal adipose tissue with significantly altered fatty acid release from white adipose tissue upon fasting (16). This effect is believed to be mediated by Sirt1 inhibition of peroxisome proliferative-activated receptor (PPAR)-$\gamma$ expression (16). Because PPAR-$\gamma$ is a major inhibitor of osteoblastogenesis (17), we anticipated significant skeletal changes in *Sirt1*$^{+/-}$ mice and compared them with their *Sirt1*$^{+/+}$ wild type (WT) littermates.

Our results demonstrate that Sirt1 is a major regulator of bone mass. Importantly, we uncover *Sost* as a novel target for Sirt1. Sirt1 represses the expression of *Sost*, encoding for sclerostin, a critical inhibitor of bone formation, by modifying histone 3 acetylation at the *Sost* promoter. These findings suggest that Sirt1 is a potential target to promote bone formation as an anabolic approach to the treatment of osteoporosis.

## Materials and Methods

### Animal experimentation

*Sirt1*$^{+/-}$ mice in a 129/Sv background and the littermates of the parental wild-type inbred strain were used (16). To label the bone-forming surfaces, the mice were injected sc with calcein at 15 mg/kg, 7 and 2 d before they were killed. At the time the mice were killed, blood was collected and the femurs and L4 were removed for primary bone marrow cultures, histomorphometry, and microcomputed tomography ($\mu$CT) imaging. Animal studies were approved by the Hebrew University Committee on the Use and Care of Animals. Unless otherwise stated, we performed all experiments in 12-wk-old *Sirt1*$^{+/-}$ and WT female mice.

### $\mu$CT and bone histomorphometry

Whole femora and the fourth vertebra were examined by a $\mu$CT system (Desktop $\mu$CT 42; Scanco, Brüttisellen, Switzerland). Femoral trabecular bone in the secondary spongiosa in the distal metaphysis and cortical bone in the middiaphyseal segment were analyzed. For histomorphometric analyses, femurs were embedded undecalcified in polymethylmethacrylate. The mineralizing surface and mineral apposition rate were measured 0.75–2.25 mm proximal of the distal growth plate. The analysis was performed using IMAGE-PRO EXPRESS 4.0 software (Media Cybernetics, Silver Spring, MD). Static parameters of bone formation and resorption were measured in an area between 181 and 1080 $\mu$m from the growth plate, using an OsteoMeasure morphometry system (Osteometrics, Atlanta, GA) as previously described (18).

### Biochemical markers

Serum CrossLaps (C terminal telopeptides, a bone resorption marker), procollagen 1 N-terminal peptide (a bone formation marker), IGF-I, and 25-hydroxyvitamin D$_3$ were measured with IDS kits (Immunodiagnostic Systems Ltd., Boldon Business Park, UK) and 17$\beta$-estradiol with an ALPCO Diagnostics kit (ALPCO Diagnostics, Salem, NH).

### C3H10T1/2 cell line

Sirt1 overexpression in the murine mesenchymal embryonic fibroblast stem cell line C3H10T1/2 was modified through retroviral infection with pBABE-*Sirt1*.

### Primary bone marrow cell cultures

Bone marrow cells were harvested from femurs of 12-wk-old *Sirt1*$^{+/-}$ and WT female or male mice. The femurs were removed and cleaned of connective tissue, the ends were cut, and the marrow was flushed with $\alpha$-MEM/15% fetal calf serum. Single-cell suspensions were prepared in $\alpha$-MEM by drawing the cells several times through graded needles. Cell density was determined by counting in a hemocytometer. Nonadherent cells were removed after 24 h, and the medium was changed every 3 d. The cells were plated in a density of $10 \times 10^6$ cells in a 60-mm dish for RNA, protein purification, alkaline phosphatase activity, and mineralized nodule formation. For the experiment with the antisclerostin antibody, $6 \times 10^6$ cells/well were plated in six-well-plates.

### Osteogenic and adipogenic conditions

Primary bone marrow-derived cells were induced to osteogenesis by $\alpha$-MEM/15% fetal calf serum/50 $\mu$g/ml ascorbic acid/10 mM $\beta$-glycerophosphate. Alkaline phosphatase activity was determined 7 d after induced osteogenesis (Sigma-Aldrich, St. Louis, MO; catalog no. N2765 and N1048). Mineralized nodule formation was assessed on d 14 by Von Kossa staining, and the fraction of mineralized area was quantified by ImageJ (National Institutes of Health, Bethesda, MD). A sclerostin-neutralizing monoclonal antibody, kindly provided by Amgen, was added at 10 $\mu$g/ml beginning on d 0 and on each media change day thereafter. C3H10T1/2 cells were induced to osteogenesis with 0.1 nM dexamethasone/50 $\mu$g/ml ascorbic acid/10 mM $\beta$-glycerophosphate.

Adipogenesis was induced by 10 $\mu$g/ml insulin/50 $\mu$M dexamethasone/100 $\mu$M indomethacin/500 $\mu$M 3-isobutyl-1-methylxanthine and maintained in 10 $\mu$g/ml insulin/50 $\mu$M dexametha-

sone/5 $\mu$M rosiglitazone (19). Adipocyte number was determined by Oil-Red-O staining.

## Gene expression analyses

RNA was extracted, reverse transcribed, and analyzed with SYBR Green-based RT-PCR. For the gene array assay, RNA was extracted and reverse transcribed using RT$^2$ first-strand kit (SABiosciences, Frederick, MD). Analysis of the mouse osteogenesis signaling pathway was performed with the RT$^2$ Profiler PCR array (SABiosciences). The antibodies, $\alpha$-Sir2 (Upstate Biotechnology, Charlottesville, VA), $\alpha$-sclerostin (Abcam, Cambridge, UK), $\alpha$-glyceraldehyde-3-phosphate dehydrogenase (Abcam), and $\alpha$-HSP90 (BD Transduction Laboratories, Franklin Lakes, NJ) were used for Western blotting.
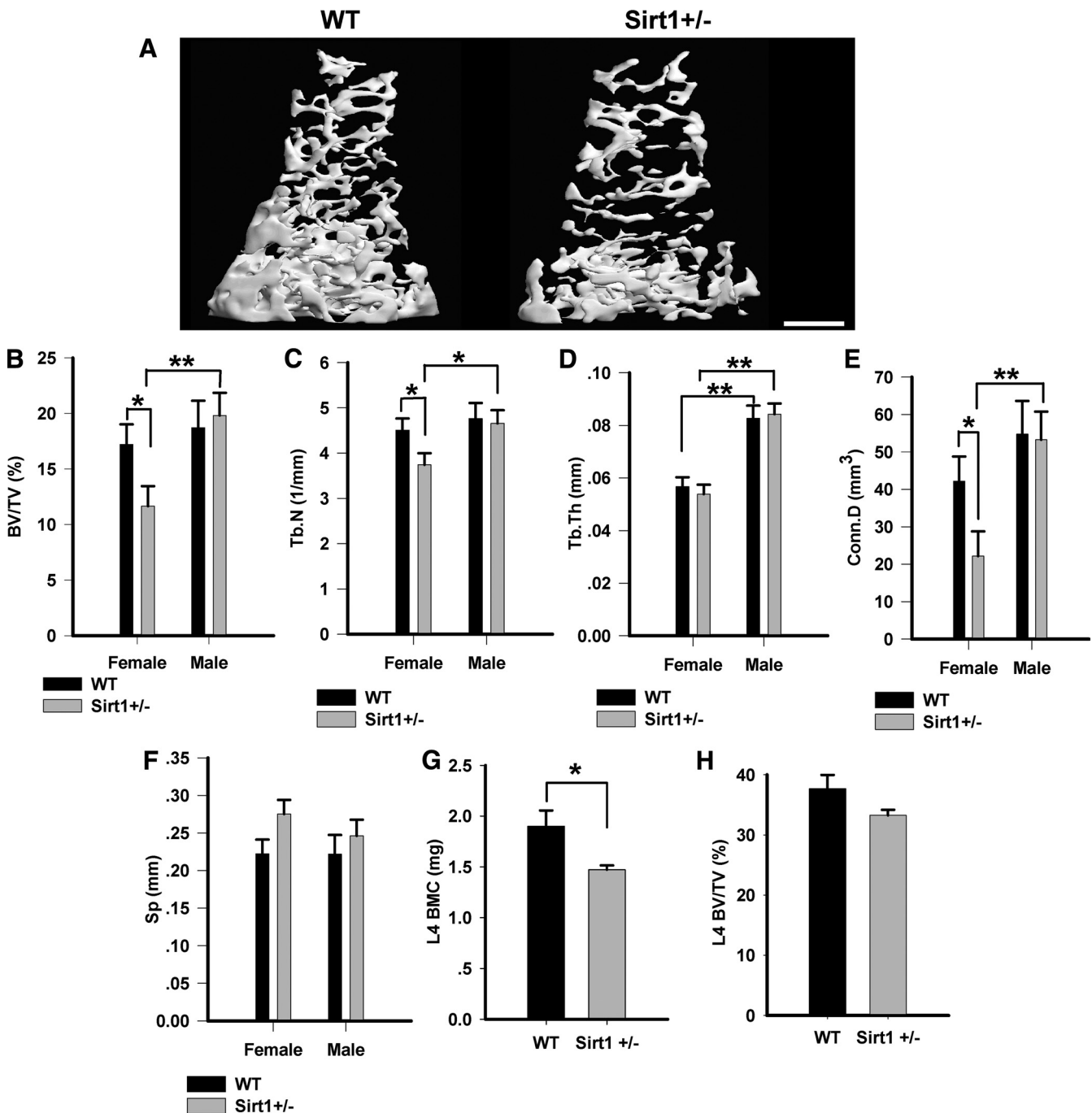


**FIG. 1.** Bone mass in Sirt1$^{+/-}$ and WT mice. A–F, $\mu$CT images and analyses in distal femurs of 12-wk-old female and male Sirt1$^{+/-}$ and WT mice (n = 9 for female, n = 5 and 7 for male). A, $\mu$CT images of distal femoral metaphyseal trabecular bone in 12-wk-old Sirt1$^{+/-}$ and WT female mice. Scale bar, 0.5 mm. BV/TV, bone volume/total volume (B); Tb.N, Trabecular number (C); Tb.Th, trabecular thickness (D); Conn.D, connectivity density (E); Sp, trabecular spacing (F). G and H, Vertebral (L4) bone mineral content and BV/TV in 12-wk-old Sirt1$^{+/-}$ and WT female mice (n = 9). Results are mean ± SEM. Statistical analysis was performed in B–F by two-way ANOVA with sex and genotype as the independent variables followed by Student-Newman-Keuls pairwise comparisons. In G and H, the Student's $t$ test was used. *, $P < 0.05$; **, $P < 0.01$.
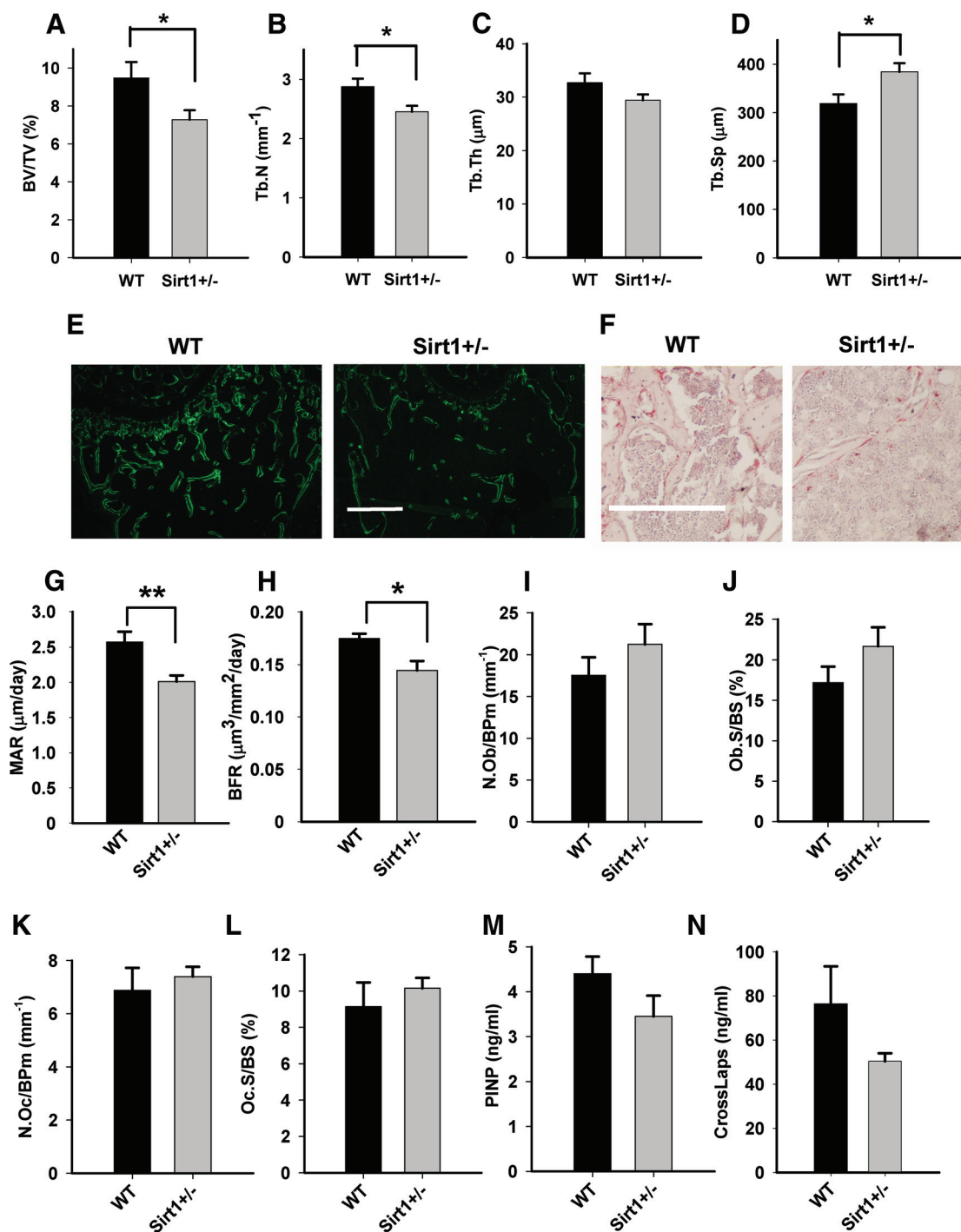
**FIG. 2.** Decreased bone formation in 12-wk-old *Sirt1*^{+/−} female mice. A–L, Histomorphometric analysis of femurs in 12-wk-old mice (n = 6–10). BV/TV, Bone volume/total volume. Tb.N, Trabecular number; Tb.Th, trabecular thickness; Tb.Sp, trabecular separation; MAR, mineral apposition rate; BFR, bone formation rate; N.Ob/Bpm, osteoblast number per bone perimeter; Ob.S/BS, osteoblast surface per bone surface, N.Oc/Bpm, osteoclast number per bone perimeter; Oc.S/Bs, osteoclast surface per bone surface. E, Fluorescent imaging of calcein incorporated into mineralizing newly formed bone. *Bar*, 200 μm. F, Tartrate-resistant acid phosphatase staining of osteoclasts in femoral trabecular bone. *Bar*, 0.5 mm. M and N, Serum levels of amino-terminal propeptide of type I procollagen (P1NP) and CrossLaps, markers of bone formation and resorption (n = 10/group). Results are mean ± SEM. Statistical analysis was performed by Student's *t* test. *, $P < 0.05$, **, $P < 0.01$ compared with WT.

## Chromatin immunoprecipitation (ChIP) analysis

Mouse *Sirt1*^{+/−} and *Sirt1*^{−/−} embryonic stem (ES) cells were cultured on gelatin to 70% confluence. Medium was replaced with 1% formaldehyde/ PBS for cross-linking and incubated for 15 min in room temperature. The cross-linking was stopped with 0.125 M glycine, followed by washes with PBS, and was continued according to the manufacturer's ChIP assay instructions (Upstate Biotechnology). Immunoprecipitation was performed with anti-Sir2 antibody (Upstate Biotechnology) and antihistone 3 at lysine 9 (H3K9)-Ac antibody (Millipore, Billerica, MA).

ChIP output was analyzed by RT-PCR and normalized by input. Enrichment of Sirt1 on nine *Sost* promoter segments was calculated by RT-PCR relative to the −53 to –173 primer. Major satellite repeats DNA sequence was used as a positive control. Enrichment of H3K9Ac on nine *Sost* promoter segments in *Sirt1*$^{-/-}$ compared with *Sirt1*$^{+/-}$ ES cells was calculated by RT-PCR. Studies were performed in triplicates. The experiment was repeated three times in three different cell preparations.

### Down-regulation of *Sost*

Bone marrow stromal mesenchymal stem cells (BM-MSC) derived from 12-wk-old female *Sirt1*$^{+/-}$ mice were transfected with small interfering RNA (siRNA)-*Sost* (Sigma) or siRNA control, using Lipofectamine RNAiMAX (Invitrogen, Carlsbad, CA). Protein and RNA were collected 6 d after induced osteogenesis. Data presented are the mean of three experiments.

### Statistical analysis

Data are presented as mean ± sem. Differences of $P < 0.05$ were considered significant. Statistical analysis was performed using SigmaPlot 11 analytical software (Systat Software, Inc., Chicago, IL).

## Results

### *Sirt1*$^{+/-}$ female mice exhibit low bone mass

Twelve-week-old *Sirt1*$^{+/-}$ female mice exhibited a substantial reduction in bone mass compared with their WT littermates. There was a 30% decrease in femoral bone volume fraction (BV/TV) as a result of reduced trabecular number with no significant change in trabecular thickness, leading to decreased connectivity (Fig. 1, A–F). Vertebral (L4) bone mineral content was reduced as well (Fig. 1G). There was no statistically significant difference in L4 BV/TV (Fig. 1H). There were no significant differences in femoral length or body weight between *Sirt1*$^{+/-}$ and WT mice (15.1 ± 0.1 *vs.* 15.5 ± 0.19 mm and 20.2 ± 0.65 *vs.* 20.4 ± 0.62 g in *Sirt1*$^{+/-}$ and WT mice, respectively), and bone indices were similar at age 5 wk (Supplemental Table 1, published on The Endocrine Society's Journals Online web site at http://endo.endojournals.org), suggesting no major effects on growth. No differences in femoral cortical bone thickness were detected at age 12 wk. At age 7 months, a significant reduction in cortical thickness was observed in *Sirt1*$^{+/-}$ compared with WT female mice (0.297 ± 0.008 *vs.* 0.327 ± 0.010 mm in *Sirt1*$^{+/-}$ and WT mice, respectively, $P = 0.046$). The decrease in bone mass detected by μCT imaging was further confirmed by histology (Fig. 2, A–D). In males, no differences in bone indices between *Sirt1*$^{+/-}$ and WT mice were found at age 5 wk and 3 months (Supplemental Table 1 and Fig. 1, B–F).

### Decreased bone formation in *Sirt1*$^{+/-}$ female mice

To dissect the mechanism of reduced bone mass in *Sirt1*$^{+/-}$ mice, we first confirmed that Sirt1 is expressed in bone. Sirt1 was detected in BM-MSC and whole tibial extracts (see Fig. 5B and Supplemental Fig. 1). Bone formation and resorption were evaluated *in vivo*. Dynamic histomorphometric analysis in the distal metaphyseal femoral bone revealed a decrease in bone formation as indicated by reduced calcein-labeling, mineral apposition rate and bone formation rate (Fig. 2, E, G, and H). Importantly, mineral apposition rate, which measures the osteogenic activity per osteoblast, was reduced, suggesting reduced osteoblast function. Osteoblast number per bone perimeter and osteoblast surface per bone surface were not different in *Sirt1*$^{+/-}$ compared with WT mice (Fig. 2, I and J). Osteoclast number per bone perimeter and osteoclast surface per bone surface were not significantly different in *Sirt1*$^{+/-}$ compared with WT mice (Fig. 2, F, K, and L). Serum amino-terminal propeptide of type I procollagen was not statistically significantly different in *Sirt1*$^{+/-}$ compared with WT mice ($P = 0.09$) (Fig. 2M). Serum CrossLaps was also not statistically significantly different in *Sirt1*$^{+/-}$ compared with WT mice (Fig. 2N). Taken together, these findings suggest that decreased bone formation is a major contributor to the low bone mass phenotype observed in *Sirt1*$^{+/-}$ female mice. We therefore focused our subsequent efforts on the mechanisms of reduced bone formation in this mouse model. No significant differences in biochemical indices of bone metabolism, including serum Ca, phosphorus, 25-hydroxyvitamin D$_3$, IGF-I, and 17β-estradiol, were detected between *Sirt1*$^{+/-}$ and WT mice (Table 1).

In support of the *in vivo* data, despite plating equal numbers of marrow cells, a 50% reduction in alkaline phosphatase activity and a strikingly reduced number of von Kossa positively stained mineralized nodules were observed in *Sirt1*$^{+/-}$ compared with WT-derived BM-MSC

**TABLE 1.** Serum biochemical indices in 12-wk-old female *Sirt1*$^{+/-}$ and WT mice

|  | WT | *Sirt1*$^{+/-}$ | *P* value |
|---|---|---|---|
| Calcium (mmol/liter) | 2.0 ± 0.2 | 2.2 ± 0.1 | 0.86 |
| Phosphorus (mmol/liter) | 2.9 ± 0.5 | 2.9 ± 0.4 | 0.96 |
| Creatinine (μmol/liter) | 45.6 ± 7.4 | 55.3 ± 3.0 | 0.16 |
| IGF-I (ng/ml) | 328.4 ± 10.3 | 319.3 ± 8.2 | 0.5 |
| 25-Hydroxyvitamin D$_3$ (nmol/liter) | 131.5 ± 6.5 | 131.0 ± 6.7 | 0.96 |
| 17β-Estradiol (pg/ml) | 41.6 ± 8.5 | 36.3 ± 5.7 | 0.97 |

Serum biochemical indices in 12-wk-old female *Sirt1*$^{+/-}$ and WT mice. Serum levels of calcium, phosphorus, creatinine, IGF-I, 25-hydroxyvitamin D$_3$, and 17β-estradiol are shown. Data are mean ± sem obtained from 10 mice in each group.

induced to osteogenesis (Fig. 3, A and B). RUNX2 mRNA expression was not different in $Sirt1^{+/-}$ compared with WT-derived BM-MSC induced to osteogenesis, consistent with no effect of $Sirt1$ haplo-insufficiency on osteoblast number (Fig. 3C). A significantly reduced mRNA expression of the osteoblastic markers bone sialoprotein, osteocalcin, and type 1 collagen was found in $Sirt1^{+/-}$ BM-MSC induced to osteogenesis (Fig. 3C), supporting the

notion of reduced osteoblast activity. A reciprocal effect was observed in C3H10T1/2 cells overexpressing Sirt1 in which a 50% increase in alkaline phosphatase activity was found (Fig. 3, D and E).

Of note, an increase in adipogenesis was observed in $Sirt1^{+/-}$-derived BM-MSC induced to adipogenesis compared with WT stromal mesenchymal stem cells as indicated by increased number of Oil-Red-O-stained
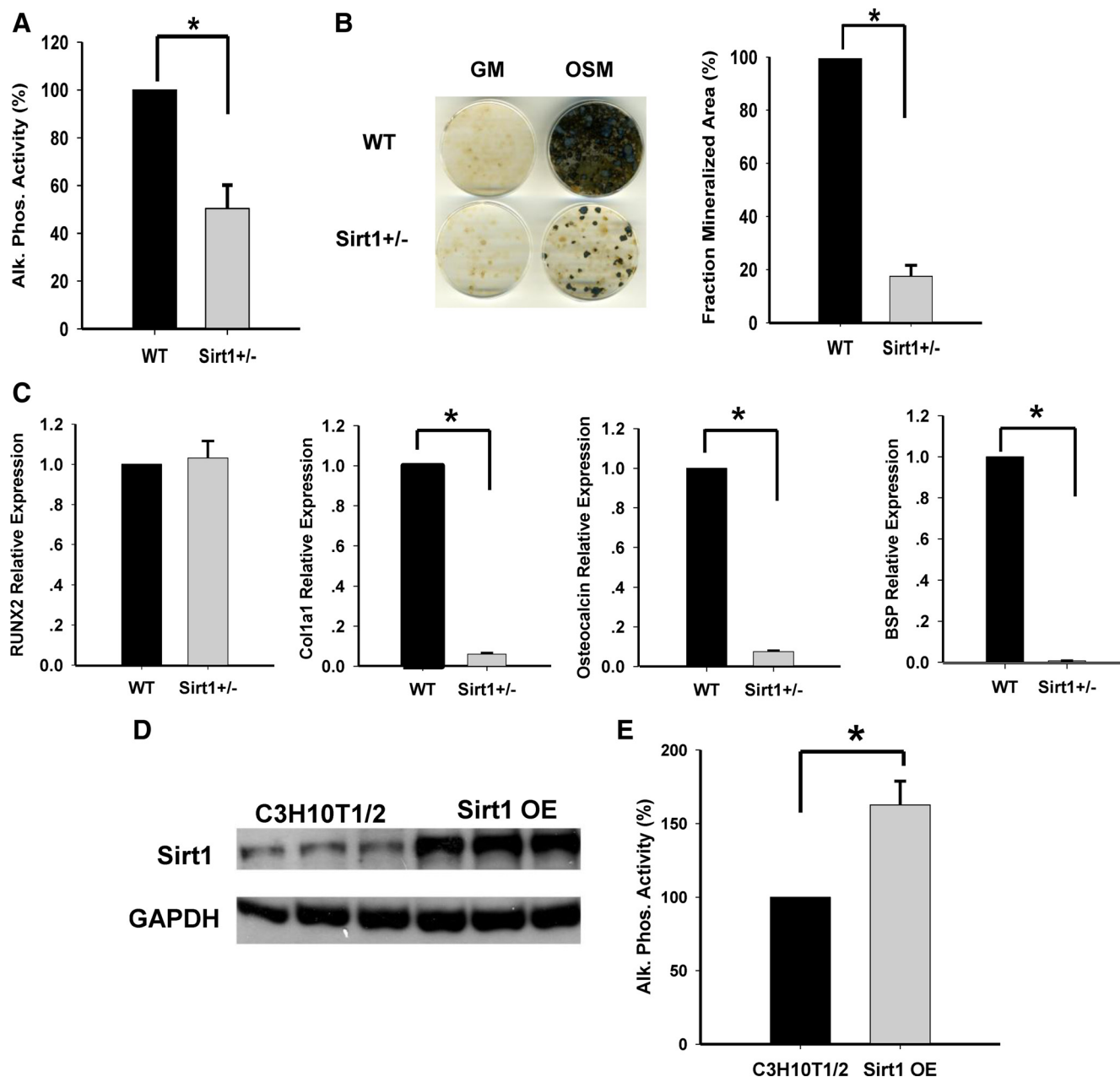


**FIG. 3.** Decreased osteoblast activity in bone marrow-derived mesenchymal stem cells obtained from $Sirt1^{+/-}$ and WT female mice. A, Alkaline phosphatase (Alk. Phos.) activity (n = 3). B, von Kossa positively stained mineralized area in growing (GM) and osteogenic medium (OSM) (×100) (quantified in four wells per condition from three different preparations). C, mRNA expression of runt-related transcription factor (RUNX)-2 48 h after induced osteogenesis. Results are relative to hypoxanthine-guanine phosphoribosyl transferase (HPRT). Collagen type 1 (Col1a1), osteocalcin, and bone sialoprotein (BSP) mRNA expression 6 d after induced osteogenesis is shown. Results are relative to ubiquitin C (UBC) (n = 3). Sirt1 and glyceraldehyde-3-phosphate dehydrogenase (GAPDH) protein levels (D) and alkaline phosphatase activity (E) (*right panel*) in Sirt1-overexpressing C3H10T1/2 and control cells. Results are mean ± SEM (n = 3). Statistical analysis was performed by Student's $t$ test. *, $P < 0.05$ compared with WT or C3H10T1/2.
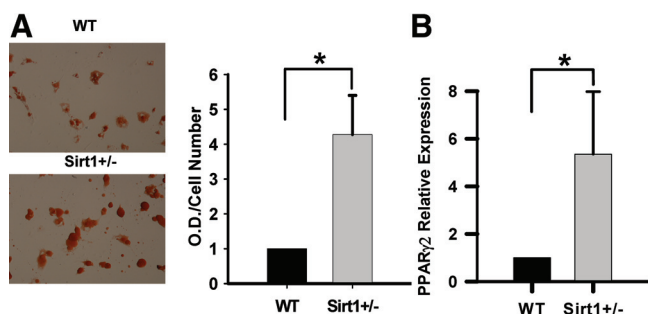
**FIG. 4.** Increased adipogenesis in bone marrow-derived mesenchymal stem cells obtained from *Sirt1*$^{+/-}$ and WT 12-wk-old female mice. A, Oil-Red-O positively stained adipocytes in *Sirt1*$^{+/-}$- and WT-derived BM-MSC induced to adipogenesis. Results are mean ± SEM of OD (n = 4). B, PPARγ2 mRNA levels in *Sirt1*$^{+/-}$-and WT-derived BM-MSC induced to adipogenesis. Results are relative to hypoxanthine-guanine phosphoribosyl transferase (HPRT). Results are mean ± SEM (n = 3). Statistical analysis was performed by Student's *t* test. *, $P < 0.05$ compared with WT.

adipocytes and higher PPARγ2 mRNA expression (Fig. 4, A and B).

### Sirt1 is a negative regulator of *Sost*

To investigate the mechanism by which Sirt1 affects bone formation, we looked for an inhibitor of bone formation that is up-regulated in the absence of Sirt1. Because Sirt1 was shown to regulate gene expression, we took an unbiased gene array approach to identify candidate genes. Gene expression in female *Sirt1*$^{+/-}$- and WT-derived BM-MSC induced to osteogenesis was compared using an osteogenesis microarray. Ten genes were differentially expressed (>3-fold change) in *Sirt1*$^{+/-}$-derived cells (Supplemental Table 2). The biggest difference was observed for *Sost* (>14-fold expression in *Sirt1*$^{+/-}$ derived cells). Based on the known inhibitory effect of sclerostin on bone formation and given that high levels of *Sost* expression could explain the phenotype observed in our *Sirt1*$^{+/-}$ mice, we decided to focus our studies on this particular gene. Aligned with the gene expression data, sclerostin was increased in whole femoral bone extracts obtained from *Sirt1*$^{+/-}$ mice and in *Sirt1*$^{+/-}$-derived BM-MSC (Fig. 5, A–C). Interestingly, increased sclerostin was also found in *Sirt1*$^{+/-}$ male-derived BM-MSCs (Fig. 5D). However, no difference in alkaline phosphatase activity between male *Sirt1*$^{+/-}$ and WT BM-MSC induced to osteogenesis was found (data not shown). Conversely, a significantly lower sclerostin was observed in Sirt1-overexpressing C3H10T1/2 cells induced to osteogenesis (Fig. 5E). These results suggest that Sirt1 down-regulates sclerostin.

Previous work has demonstrated that Sirt1 directly regulates gene expression acting as a histone deacetylase (20). To investigate whether this was the case for *Sost*, a ChIP assay was performed with an anti-Sirt1 antibody in mouse ES cells. These cells exhibit undetectable sclerostin level, and therefore, we hypothesized that expression of *Sost* is repressed in these cells. *Sirt1*$^{-/-}$ ES cells were used as negative controls (14). RT-PCR assays using primers that cover eight consecutive segments in the 5′ regulatory region of the *Sost* promoter were performed. Strikingly, we found significant Sirt1 binding to the *Sost* promoter in a region encompassing 760-1940 bp upstream of the start codon (Fig. 5F). Corroborating these data, no binding of Sirt1 to this region was detected in *Sirt1*$^{-/-}$ ES cells (Supplemental Table 3). These findings suggest that Sirt1 specifically binds to the *Sost* promoter and likely contributes to its silencing.

We next asked whether Sirt1 functions as a histone deacetylase at the *Sost* promoter. H3K9 was previously identified as specific Sirt1 target (21). To test whether this was the case for *Sost*, a ChIP assay was performed with anti-H3K9Ac antibody. *Sirt1*$^{-/-}$ ES cells exhibited a marked increase in H3K9 acetylation at the *Sost* promoter compared with WT cells, peaking at 930-1115 bp upstream of the start codon, at which maximal Sirt1 binding occurred (Fig. 5G). Together these results provide strong support for the notion that Sirt1 suppresses *Sost* expression by modifying H3K9 acetylation at its promoter.

To confirm that increased sclerostin is a major contributor to reduced osteoblast activity, a sclerostin-neutralizing antibody and *Sost* down-regulation by siRNA were used in *Sirt1*$^{+/-}$ marrow-derived osteoblasts. Treatment with the sclerostin antibody not only restored von Kossa-positive-stained mineralized nodule formation but overcorrected it, suggesting a higher basal sclerostin level in *Sirt1*$^{+/-}$ mice (Fig. 5H). *Sost* down-regulation tripled mRNA levels of osteocalcin and bone sialoprotein (Fig. 5I). These data strongly suggest that decreased osteoblast activity in female-derived osteoblasts is due to increased sclerostin.

### Discussion

This study demonstrates for the first time a role for Sirt1 in bone and shows that Sirt1 is a regulator of bone mass. *Sirt1*$^{+/-}$ female mice exhibit a dramatic decrease in bone mass as a result of reduced bone formation. Importantly, we uncovered a link between Sirt1 and *Sost*, which encodes for sclerostin, a critical inhibitor of bone formation, and demonstrate that *Sost* is a novel bone-specific target of Sirt1. *Sost* gene expression is negatively regulated by Sirt1 through deacetylation of H3K9 in the promoter region.

Sclerostin, a secreted cysteine-knot protein with homology to the differential screening-selected gene aberrative in neuroblastoma family of bone morphogenic protein
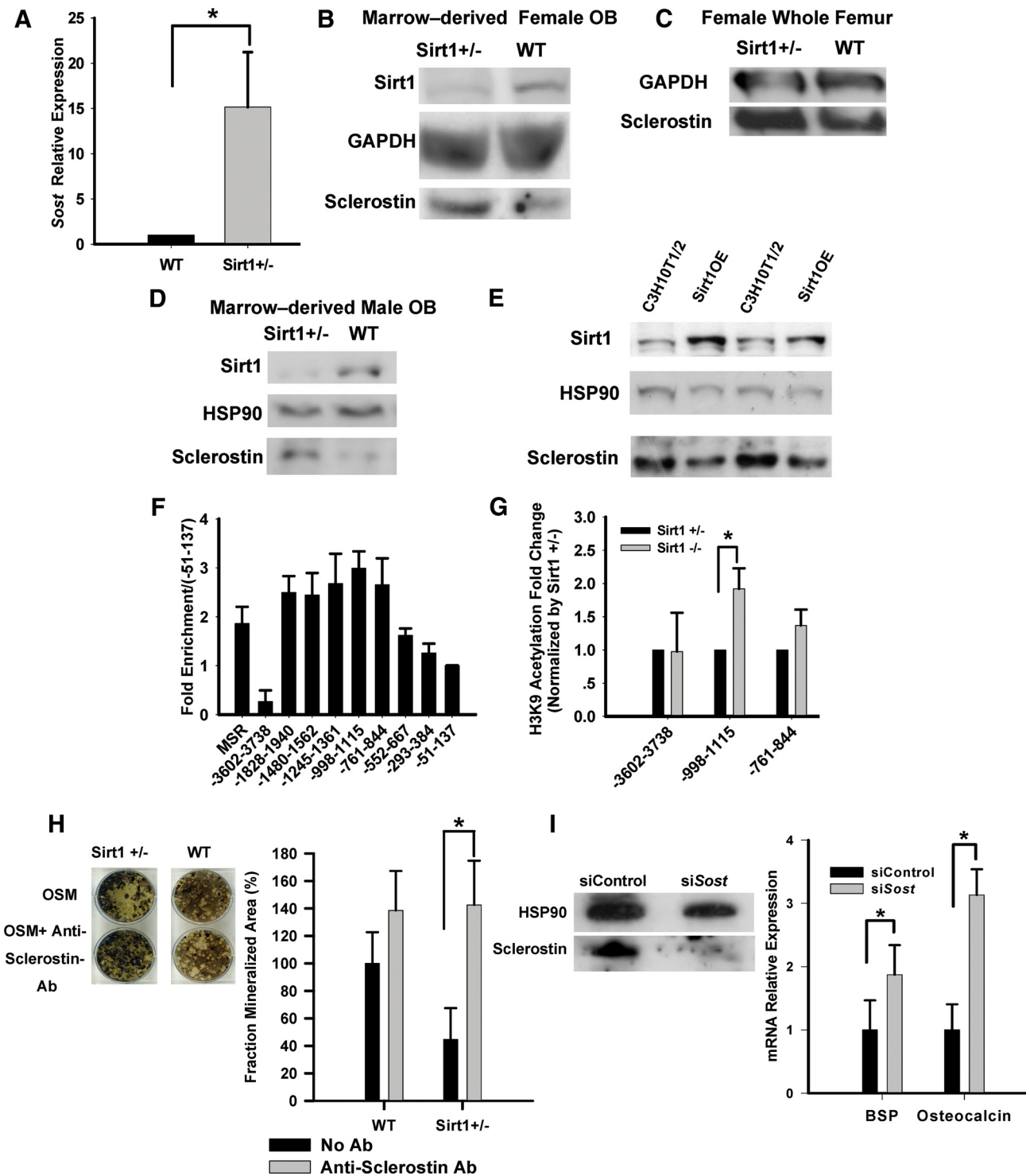
**FIG. 5.** Sirt1 is a negative regulator of *Sost*. A, Increased mRNA expression of *Sost* in *Sirt1$^{+/-}$* bone marrow-derived osteoblasts. Results are relative to hypoxanthine-guanine phosphoribosyl transferase (HPRT) (n = 3). *, $P < 0.05$. B–D, Increased sclerostin levels in female *Sirt1$^{+/-}$* compared to WT bone marrow-derived osteoblasts and whole femur extracts (B and C) and male *Sirt1$^{+/-}$* compared to WT bone marrow-derived osteoblasts (D). E, Sclerostin in Sirt1 overexpressing C3H10T1/2 and control cells on d 6 after induced osteogenesis (n = 3 for all Western data). F, ChIP assay using anti-Sirt1 antibody in *Sirt1$^{+/-}$* ES cells. Real-time PCR analysis of Sirt1 binding to the *Sost* promoter region. Results are relative enrichment compared with the −51–137 primer. Major satellite repeats DNA sequence (MSR) and a primer at −3600 to −3738 served as positive and negative controls, respectively. G, ChIP assay using antibody against acetylated histone H3K9 in *Sirt1$^{+/-}$* and *Sirt1$^{-/-}$* ES cells. Statistical analysis was performed by Student's $t$ test (for all ChIP data, n = 3). H, von Kossa positively stained mineralized area in *Sirt1$^{+/-}$* and WT BM-MSC induced to osteogenesis (OSM) with and without a sclerostin-neutralizing antibody. Results are mean ± SEM (n = 4). Statistical analysis was performed by two-way ANOVA with genotype and treatment as independent variables followed by Student-Newman-Keuls pairwise comparison. Ab, Antibody. *, $P < 0.05$. I, Sclerostin levels and mRNA levels of bone sialoprotein (BSP) and osteocalcin in *Sirt1$^{+/-}$*-derived osteoblasts transfected with *Sost* or control siRNA for down-regulation of *Sost*. Results are relative to UBC (n = 3).

antagonists, is a major inhibitor of bone formation (22). In adult bone, it is constitutively expressed by osteocytes, a final differentiated cell of the osteoblast lineage (23). Sclerostin is detected in not only osteocytes but also in marrow stromal cells, osteoclast precursors, and osteoblasts during embryonic bone development (24–26). Its role in bone biology was first appreciated when excessive bone mass was observed in patients with Van Buchem's disease or sclerosteosis in whom mutations or deletions in the *Sost* gene were identified (27–30). Its physiological importance was further supported by the high bone mass phenotype found in sclerostin-null mice (31), and a low bone mass phenotype in sclerostin overexpressing mice (32).

Sclerostin's mechanism of action is not fully understood. It was shown to disrupt the formation of the Wnt-induced frizzled-low-density lipoprotein receptor-related protein 5 (LRP5) and its corecptor LRP6 complex (33–35). But the mechanism by which its binding to LRP5/6 interferes with canonical Wnt signaling and bone formation remains unknown. Data regarding a direct effect of sclerostin on downstream targets in the canonical Wnt pathway such as active $\beta$-catenin and its targets T-cell factor/lymphoid enhancer binding factor 1 have been inconclusive. Importantly, bone mass and strength in aged ovariectomized rats (36) and aged male rats (37) are restored by the administration of a sclerostin-neutralizing antibody. Moreover, an impressive increase in spine and hip bone mineral density in postmenopausal women treated with an antisclerostin monoclonal antibody was recently reported (38).

The regulatory control of *Sost* expression is only partially known. Mechanical loading reduces *Sost* mRNA expression and sclerostin levels in osteocytes, whereas unloading leads to an increase (23, 39, 40). The anabolic effect of PTH was shown to be mediated, in part, by suppressing *Sost* expression. Indeed, a blunted anabolic effect of PTH in *Sost*-deficient mice was observed (41). A role for estrogen in the regulation of sclerostin levels has been implicated by the finding of increased serum sclerostin in postmenopausal compared with premenopausal women (42) and a reversal upon estrogen replacement (43). Oncostatin M was reported to inhibit sclerostin production in a stromal cell line and in primary murine osteoblast cultures (44). Our study indicates that Sirt1 is a novel negative regulator of *Sost* and its product sclerostin by epigenetic silencing of *Sost* gene expression. It will be important to test in future studies whether *Sirt1*$^{+/-}$ female mice are more susceptible to ovariectomy-induced bone loss. Moreover, whether Sirt1-mediated changes in *Sost* transcription are involved in the pathogenesis of osteoporosis and age-associated bone loss awaits further investigation.

Our results indicate that the effect of Sirt1 deficiency on femoral bone mass is more pronounced in females than males. Our findings of a sexual dimorphic phenotype are consistent with other *Sirt1*-related transgenic mouse models. Thus, female but not male mice lacking Sirt1 in proopiomelanocortin neurons display a striking hypersensitivity to diet-induced obesity (45). In addition, female but not male mice lacking nicotinamide phosphoribosyltransferase (*Nampt*), a key enzyme in the biosynthesis of the oxidation of nicotinamide adenine dinucleotide, an essential cofactor for Sirt1 activity, showed impaired glucose tolerance and reduced insulin secretion (46). A limitation of this work is lack of data on vertebral bone mass in *Sirt1*$^{+/-}$ and WT male mice. Because there was no difference in femoral bone indices between *Sirt1*$^{+/-}$ and WT male mice and the differences in vertebral indices in females were small, we anticipated no difference in spinal bone mass in *Sirt1*$^{+/-}$ and WT male mice.

To better understand the underlying mechanism of this dimorphic effect on bone mass, we asked whether Sirt1 deficiency affects sclerostin in males as it does in females. Interestingly, similar to females, the sclerostin level was increased in male *Sirt1*$^{+/-}$ compared with WT mice (Fig. 5D), suggesting that Sirt1 represses sclerostin in both genders. These findings are consistent with the data of Ramadori *et al.* (45), who reported that Sirt1 deletion in proopiomelanocortin neurons alters uncoupling protein-1 and tyrosine hydroxylase protein levels in perigonodal white adipose tissue in both females and males, yet a body weight phenotype was observed in females but not males. Thus, we speculate that factors downstream of sclerostin are affected by sex.

In summary, our study uncovers a role for Sirt1 as a regulator of bone mass and demonstrates a novel Sirt1-*Sost* connection, revealing that Sirt1 is a transcriptional repressor of *Sost*. The hypothesis that Sirt1-mediated epigenetic changes in *Sost* transcription are involved in osteoporosis awaits further investigation. It is possible that Sirt1 targets, in addition to *Sost*, also contribute to the phenotype observed in *Sirt1*$^{+/-}$ mice. Our findings have important clinical implications: they suggest that specific Sirt1 activators may stimulate bone formation, and provide a new strategy for generating a much needed anabolic therapy for osteoporosis.

## Acknowledgments

# References

1. Finkel T, Deng CX, Mostoslavsky R 2009 Recent progress in the biology and physiology of sirtuins. Nature 460:587–591

2. Imai S, Armstrong CM, Kaeberlein M, Guarente L 2000 Transcriptional silencing and longevity protein Sir2 is an NAD-dependent histone deacetylase. Nature 403:795–800

3. Lin SJ, Defossez PA, Guarente L 2000 Requirement of NAD and SIR2 for life-span extension by calorie restriction in Saccharomyces cerevisiae. Science 289:2126–2128

4. Bordone L, Cohen D, Robinson A, Motta MC, van Veen E, Czopik A, Steele AD, Crowe H, Marmor S, Luo J, Gu W, Guarente L 2007 SIRT1 transgenic mice show phenotypes resembling calorie restriction. Aging Cell 6:759–767

5. Donmez G, Wang D, Cohen DE, Guarente L 2010 SIRT1 suppresses $\beta$-amyloid production by activating the $\alpha$-secretase gene ADAM10. Cell 142:320–332

6. Elbaz A, Rivas D, Duque G 2009 Effect of estrogens on bone marrow adipogenesis and Sirt1 in aging C57BL/6J mice. Biogerontology 10: 747–755

7. Bäckesjö CM, Li Y, Lindgren U, Haldosén LA 2006 Activation of Sirt1 decreases adipocyte formation during osteoblast differentiation of mesenchymal stem cells. J Bone Miner Res 21:993–1002

8. Bäckesjö CM, Li Y, Lindgren U, Haldosén LA 2009 Activation of Sirt1 decreases adipocyte formation during osteoblast differentiation of mesenchymal stem cells. Cells Tissues Organs 189:93–97

9. He X, Andersson G, Lindgren U, Li Y 2010 Resveratrol prevents RANKL-induced osteoclast differentiation of murine osteoclast progenitor RAW 264.7 cells through inhibition of ROS production. Biochem Biophys Res Commun 401:356–362

10. Shakibaei M, Buhrmann C, Mobasheri A 2011 Resveratrol-mediated SIRT-1 interactions with p300 modulate receptor activator of NF-$\kappa$B ligand (RANKL) activation of NF-$\kappa$B signaling and inhibit osteoclastogenesis in bone-derived cells. J Biol Chem 286:11492–11505

11. Pearson KJ, Baur JA, Lewis KN, Peshkin L, Price NL, Labinskyy N, Swindell WR, Kamara D, Minor RK, Perez E, Jamieson HA, Zhang Y, Dunn SR, Sharma K, Pleshko N, Woollett LA, Csiszar A, Ikeno Y, Le Couteur D, Elliott PJ, Becker KG, Navas P, Ingram DK, Wolf NS, Ungvari Z, Sinclair DA, de Cabo R 2008 Resveratrol delays age-related deterioration and mimics transcriptional aspects of dietary restriction without extending life span. Cell Metab 8:157–168

12. Bowers JL, Tyulmenkov VV, Jernigan SC, Klinge CM 2000 Resveratrol acts as a mixed agonist/antagonist for estrogen receptors $\alpha$ and $\beta$. Endocrinology 141:3657–3667

13. Liu M, Wilk SA, Wang A, Zhou L, Wang RH, Ogawa W, Deng C, Dong LQ, Liu F 2010 Resveratrol inhibits mTOR signaling by promoting the interaction between mTOR and DEPTOR. J Biol Chem 285:36387–36394

14. Cheng HL, Mostoslavsky R, Saito S, Manis JP, Gu Y, Patel P, Bronson R, Appella E, Alt FW, Chua KF 2003 Developmental defects and p53 hyperacetylation in Sir2 homolog (SIRT1)-deficient mice. Proc Natl Acad Sci USA 100:10794–10799

15. McBurney MW, Yang X, Jardine K, Hixon M, Boekelheide K, Webb JR, Lansdorp PM, Lemieux M 2003 The mammalian SIR2$\alpha$ protein has a role in embryogenesis and gametogenesis. Mol Cell Biol 23:38–54

16. Picard F, Kurtev M, Chung N, Topark-Ngarm A, Senawong T, Machado De Oliveira R, Leid M, McBurney MW, Guarente L 2004 Sirt1 promotes fat mobilization in white adipocytes by repressing PPAR-$\gamma$. Nature 429:771–776

17. Akune T, Ohba S, Kamekura S, Yamaguchi M, Chung UI, Kubota N, Terauchi Y, Harada Y, Azuma Y, Nakamura K, Kadowaki T, Kawaguchi H 2004 PPAR$\gamma$ insufficiency enhances osteogenesis through osteoblast formation from bone marrow progenitors. J Clin Invest 113:846–855

18. Gazzero E, Pereira RC, Jorgetti V, Olson S, Economides AN, Canalis E 2005 Skeletal overexpression of gremlin impairs bone formation and causes osteopenia. Endocrinology 146:655–665

19. Moisan A, Rivera MN, Lotinun S, Akhavanfard S, Coffman EJ, Cook EB, Stoykova S, Mukherjee S, Schoonmaker JA, Burger A, Kim WJ, Kronenberg HM, Baron R, Haber DA, Bardeesy N 2011 The WTX tumor suppressor regulates mesenchymal progenitor cell fate specification. Dev Cell 20:583–596

20. Oberdoerffer P, Michan S, McVay M, Mostoslavsky R, Vann J, Park SK, Hartlerode A, Stegmuller J, Hafner A, Loerch P, Wright SM, Mills KD, Bonni A, Yankner BA, Scully R, Prolla TA, Alt FW, Sinclair DA 2008 SIRT1 redistribution on chromatin promotes genomic stability but alters gene expression during aging. Cell 135: 907–918

21. Wang RH, Zheng Y, Kim HS, Xu X, Cao L, Luhasen T, Lee MH, Xiao C, Vassilopoulos A, Chen W, Gardner K, Man YG, Hung MC, Finkel T, Deng CX 2008 Interplay among BRCA1, SIRT1, and Survivin during BRCA1-associated tumorigenesis. Mol Cell 32: 11–20

22. Poole KE, van Bezooijen RL, Loveridge N, Hamersma H, Papapoulos SE, Löwik CW, Reeve J 2005 Sclerostin is a delayed secreted product of osteocytes that inhibits bone formation. FASEB J 19: 1842–1844

23. Lin C, Jiang X, Dai Z, Guo X, Weng T, Wang J, Li Y, Feng G, Gao X, He L 2009 Sclerostin mediates bone response to mechanical unloading through antagonizing Wnt/$\beta$-catenin signaling. J Bone Miner Res 24:1651–1661

24. Bellido T, Ali AA, Gubrij I, Plotkin LI, Fu Q, O'Brien CA, Manolagas SC, Jilka RL 2005 Chronic elevation of parathyroid hormone

in mice reduces expression of sclerostin by osteocytes: a novel mechanism for hormonal control of osteoblastogenesis. Endocrinology 146:4577–4583

25. Kamiya N, Ye L, Kobayashi T, Mochida Y, Yamauchi M, Kronenberg HM, Feng JQ, Mishina Y 2008 BMP signaling negatively regulates bone mass through sclerostin by inhibiting the canonical Wnt pathway. Development 135:3801–3811

26. Pederson L, Ruan M, Westendorf JJ, Khosla S, Oursler MJ 2008 Regulation of bone formation by osteoclasts involves Wnt/BMP signaling and the chemokine sphingosine-1-phosphate. Proc Natl Acad Sci USA 105:20764–20769

27. Balemans W, Ebeling M, Patel N, Van Hul E, Olson P, Dioszegi M, Lacza C, Wuyts W, Van Den Ende J, Willems P, Paes-Alves AF, Hill S, Bueno M, Ramos FJ, Tacconi P, Dikkers FG, Stratakis C, Lindpaintner K, Vickery B, Foernzler D, Van Hul W 2001 Increased bone density in sclerosteosis is due to the deficiency of a novel secreted protein (SOST). Hum Mol Genet 10:537–543

28. Balemans W, Patel N, Ebeling M, Van Hul E, Wuyts W, Lacza C, Dioszegi M, Dikkers FG, Hildering P, Willems PJ, Verheij JB, Lindpaintner K, Vickery B, Foernzler D, Van Hul W 2002 Identification of a 52 kb deletion downstream of the SOST gene in patients with van Buchem disease. J Med Genet 39:91–97

29. Brunkow ME, Gardner JC, Van Ness J, Paeper BW, Kovacevich BR, Proll S, Skonier JE, Zhao L, Sabo PJ, Fu Y, Alisch RS, Gillett L, Colbert T, Tacconi P, Galas D, Hamersma H, Beighton P, Mulligan J 2001 Bone dysplasia sclerosteosis results from loss of the SOST gene product, a novel cystine knot-containing protein. Am J Hum Genet 68:577–589

30. Staehling-Hampton K, Proll S, Paeper BW, Zhao L, Charmley P, Brown A, Gardner JC, Galas D, Schatzman RC, Beighton P, Papapoulos S, Hamersma H, Brunkow ME 2002 A 52-kb deletion in the SOST-MEOX1 intergenic region on 17q12–q21 is associated with van Buchem disease in the Dutch population. Am J Med Genet 110:144–152

31. Li X, Ominsky MS, Niu QT, Sun N, Daugherty B, D'Agostin D, Kurahara C, Gao Y, Cao J, Gong J, Asuncion F, Barrero M, Warmington K, Dwyer D, Stolina M, Morony S, Sarosi I, Kostenuik PJ, Lacey DL, Simonet WS, Ke HZ, Paszty C 2008 Targeted deletion of the sclerostin gene in mice results in increased bone formation and bone strength. J Bone Miner Res 23:860–869

32. Winkler DG, Sutherland MK, Geoghegan JC, Yu C, Hayes T, Skonier JE, Shpektor D, Jonas M, Kovacevich BR, Staehling-Hampton K, Appleby M, Brunkow ME, Latham JA 2003 Osteocyte control of bone formation via sclerostin, a novel BMP antagonist. EMBO J 22:6267–6276

33. Semënov M, Tamai K, He X 2005 SOST is a ligand for LRP5/LRP6 and a Wnt signaling inhibitor. J Biol Chem 280:26770–26775

34. van Bezooijen RL, Roelen BA, Visser A, van der Wee-Pals L, de Wilt E, Karperien M, Hamersma H, Papapoulos SE, ten Dijke P, Löwik CW 2004 Sclerostin is an osteocyte-expressed negative regulator of bone formation, but not a classical BMP antagonist. J Exp Med 199:805–814

35. van Bezooijen RL, Svensson JP, Eefting D, Visser A, van der Horst G, Karperien M, Quax PH, Vrieling H, Papapoulos SE, ten Dijke P, Löwik CW 2007 Wnt but not BMP signaling is involved in the inhibitory action of sclerostin on BMP-stimulated bone formation. J Bone Miner Res 22:19–28

36. Li X, Ominsky MS, Warmington KS, Morony S, Gong J, Cao J, Gao Y, Shalhoub V, Tipton B, Haldankar R, Chen Q, Winters A, Boone T, Geng Z, Niu QT, Ke HZ, Kostenuik PJ, Simonet WS, Lacey DL, Paszty C 2009 Sclerostin antibody treatment increases bone formation, bone mass, and bone strength in a rat model of postmenopausal osteoporosis. J Bone Miner Res 24:578–588

37. Li X, Warmington KS, Niu QT, Asuncion FJ, Barrero M, Grisanti M, Dwyer D, Stouch B, Thway TM, Stolina M, Ominsky MS, Kostenuik PJ, Simonet WS, Paszty C, Ke HZ 2010 Inhibition of sclerostin by monoclonal antibody increases bone formation, bone mass, and bone strength in aged male rats. J Bone Miner Res 25:2647–2656

38. Padhi D, Jang G, Stouch B, Fang L, Posvar E 2011 Single-dose, placebo-controlled, randomized study of AMG 785, a sclerostin monoclonal antibody. J Bone Miner Res 26:19–26

39. Robling AG, Niziolek PJ, Baldridge LA, Condon KW, Allen MR, Alam I, Mantila SM, Gluhak-Heinrich J, Bellido TM, Harris SE, Turner CH 2008 Mechanical stimulation of bone *in vivo* reduces osteocyte expression of Sost/sclerostin. J Biol Chem 283:5866–5875

40. Moustafa A, Sugiyama T, Saxon LK, Zaman G, Sunters A, Armstrong VJ, Javaheri B, Lanyon LE, Price JS 2009 The mouse fibula as a suitable bone for the study of functional adaptation to mechanical loading. Bone 44:930–935

41. Kramer I, Loots GG, Studer A, Keller H, Kneissel M 2010 Parathyroid hormone (PTH)-induced bone gain is blunted in SOST overexpressing and deficient mice. J Bone Miner Res 25:178–189

42. Mirza FS, Padhi ID, Raisz LG, Lorenzo JA 2010 Serum sclerostin levels negatively correlate with parathyroid hormone levels and free estrogen index in postmenopausal women. J Clin Endocrinol Metab 95:1991–1997

43. Mödder UI, Clowes JA, Hoey K, Peterson JM, McCready L, Oursler MJ, Riggs BL, Khosla S 2011 Regulation of circulating sclerostin levels by sex steroids in women and in men. J Bone Miner Res 26:27–34

44. Walker EC, McGregor NE, Poulton IJ, Solano M, Pompolo S, Fernandes TJ, Constable MJ, Nicholson GC, Zhang JG, Nicola NA, Gillespie MT, Martin TJ, Sims NA 2010 Oncostatin M promotes bone formation independently of resorption when signaling through leukemia inhibitory factor receptor in mice. J Clin Invest 120:582–592

45. Ramadori G, Fujikawa T, Fukuda M, Anderson J, Morgan DA, Mostoslavsky R, Stuart RC, Perello M, Vianna CR, Nillni EA, Rahmouni K, Coppari R 2010 SIRT1 deacetylase in POMC neurons is required for homeostatic defenses against diet-induced obesity. Cell Metab 12:78–87

46. Revollo JR, Körner A, Mills KF, Satoh A, Wang T, Garten A, Dasgupta B, Sasaki Y, Wolberger C, Townsend RR, Milbrandt J, Kiess W, Imai S 2007 Nampt/PBEF/Visfatin regulates insulin secretion in $\beta$ cells as a systemic NAD biosynthetic enzyme. Cell Metab 6:363–375